

Regular algebraic curve segments (III)—applications in interactive design and data fitting

Chandrajit L. Bajaj^{a,*}, Guoliang Xu^{b,2}

^a *Department of Computer Science University of Texas, Austin, TX 78712, USA*

^b *State Key Laboratory of Scientific and Engineering Computing, ICMSEC, Chinese Academy of Sciences, Beijing, PR China*

Received 1 January 1997; revised 7 July 2000

Abstract

In this paper (part three of the trilogy) we use low degree G^1 and G^2 continuous regular algebraic spline curves defined within parallelograms, to interpolate an ordered set of data points in the plane. We explicitly characterize curve families whose members have the required interpolating properties and possess a minimal number of inflection points. The regular algebraic spline curves considered here have many attractive features: They are easy to construct. There exist convenient geometric control handles to locally modify the shape of the curve. The error of the approximation is controllable. Since the spline curve is always inside the parallelogram, the error of the fit is bounded by the size of the parallelogram. The spline curve can be rapidly displayed, even though the algebraic curve segments are implicitly defined. © 2001 Elsevier Science B.V. All rights reserved.

Keywords: Algebraic curve; Tensor product; Polygonal chain; Parallelogram

1. Introduction

In the first two parts (Xu et al., 2000a, 2000b) of this trilogy of papers, we have introduced the concept of a discriminating family of curves by which regular algebraic curve segments are isolated. Using different discriminating families, several characterizations of the Bernstein–Bézier (BB) form of the implicitly defined real bivariate

* Corresponding author.

E-mail addresses: bajaj@ticam.utexas.edu (C.L. Bajaj), xuguo@ticam.utexas.edu (G. Xu).

¹ Supported in part by NSF grants CCR 9732306 and KDI-DMS-9873326.

² Supported by NSFC grant 19671081, currently visiting Center for Computational Visualization, UT, Austin, TX.

polynomials over the plane triangle and the parallelogram are given, so that the zero contours of the polynomials define smooth and single sheeted real algebraic (called regular) curve segments. In this part three of the trilogy of papers, we use segments of low degree algebraic curves $G_{mn}(u, v) = 0$ in tensor product BB form defined within a parallelogram or rectangle to construct G^1 and G^2 splines. A tensor product BB-form polynomial $G_{mn}(u, v) = \sum_{i=0}^m \sum_{j=0}^n b_{ij} B_i^m(u) B_j^n(v)$ of bi-degree (m, n) has total degree $m + n$, however, the class of $G_{mn}(u, v)$ is a subset of polynomials of total degree $m + n$. G^1 (respectively G^2) continuity implies curve segments share the same tangent (curvature) at join points (knots). In each of the G^1 and G^2 constructions, we develop a spline curve family whose members satisfy given interpolation conditions. Each family depends on one free parameter that is related linearly to the coefficients of $G_{mn}(u, v)$.

Prior work on using algebraic curve spline in data interpolation and fitting focus on using bivariate barycentric BB-form polynomials defined on plane triangles (see (Xu et al., 2000a, 2000b) for references). Compared with A-spline segments defined in triangular (barycentric) BB-form (Bajaj and Xu, 1999), these algebraic curve segments in tensor product form have the following distinct features:

- (1) They are easy to construct. The coefficients of the bivariate polynomial that define the curve are explicitly given.
- (2) There exist convenient geometric control handles to locally modify the shape of the curve, essential for interactive curve design.
- (3) The spline curves, for the rectangle scheme, are ε -error controllable where ε is the pre-specified width of the rectangle.
- (4) These splines curves have a minimal number of inflection points. Each curve segment of the spline curve has either no inflection points if the corresponding edge is convex, or one inflection point otherwise.
- (5) Since the required bi-degree (m, n) for G^1 and G^2 is low (in this paper, $\min\{m, n\} \leq 2$), the curve can be evaluated and displayed extremely fast. We explore both display via parameterization as well as recursive subdivision techniques (see (Peters, 1994)).
- (6) In the six spline families defined by Theorems 4.1–4.4, 5.1 and 5.2 in Sections 4 and 5, there are four cases with $\min\{m, n\} = 1$. In these cases, rational parametric expressions are easily derived. Hence, we have both the implicit form and the parametric form. Such dual form curves prove useful in several geometric design and computer graphics applications.
- (7) In treating a nonconvex edge in the triangular scheme (see (Bajaj and Xu, 1999)), we need to break the edge into two parts by inserting an artificial inflection point. In the present parallelogram or rectangle scheme, we need not divide the edge and the inflection point occurs only when necessitated by the end point interpolating conditions.

These features make these error-bounded regular algebraic spline curves promising in applications such as interactive font design, image contouring etc.

The rest of the paper is as follows. In Section 2 we show how a number of data fitting problems reduce to interpolating or approximating a polygonal chain of line segments with error bounds. Some notation and geometric conventions are introduced in Section 3. In Section 4, we discuss the problem of polygonal chain approximation by G^1 and G^2

D_4 -regular spline curves defined on parallelograms. In Section 5, we discuss the problem of polygonal chain approximation by G^1 D_3 -regular spline curves defined on rectangles. Examples are given in Section 6. Section 7 concludes the paper. Proofs are detailed in Appendix A.

2. Polygonal chains

A polygonal chain is an ordered sequence of polygonal line segments, where any three adjacent points are not collinear. Several geometry processing tasks generate polygonal chains for shape representation in $2D$. Examples include shape or font design, fitting from “noisy” data, image contouring, snakes (Kass et al., 1988) and level set methods (Sethian, 1996). In this section, we mention a few of them that have some attached error or uncertainty.

a. Noisy vertex data

The vertex data (position) comes from a multi-sampling process with possible error. The error bound ε is known in advance. Fig. 2.1 shows such a case. The white circles are the repeatedly sampled points, the black dots are approximations of the sampled points. The approximation of the point can be computed as the center of gravity or center of bounding circular fits. The polygonal chain is obtained by connecting these black dots. The spline curve to be constructed interpolates the vertices of the polygonal chain. Hence the error around each vertex is bounded by ε .

b. Noisy curve data

Suppose a curve is sampled within some ε error band around the curve. The sampled point sequence $\{v_i\}$ could be dense. To produce a polygonal chain to these points, we use a “strip pasting” technique. Choose the strip width to be no less than 2ε . Then use the minimal number of strips to cover the sample points (see Fig. 2.2). The vertices of the polygonal chain are the intersection points of two mid-lines of adjacent strips. A computational method for obtaining the minimal number strips can be found in (Bhaskaran et al., 1993). A greedy method to obtain a minimal “strip pasting” uses an adaptive piecewise linear least square fitting, starting from one end of the data. The G^1 D_3 -regular curves developed in Section 5 are very suitable to interpolate these polygonal chains.

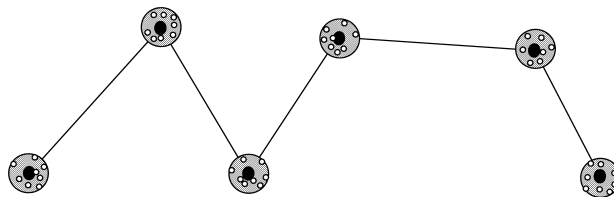


Fig. 2.1. Polygonal chain extracted from over-sampled points.

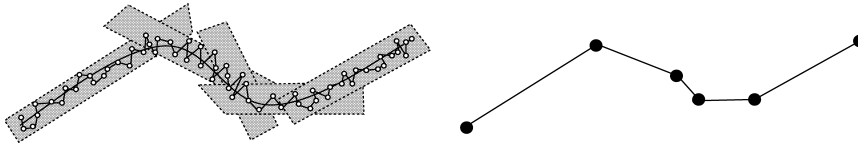


Fig. 2.2. Polygonal chain from noisy curve data and using adaptive “strip pasting”: The white circles are original sampled points with error, and the black dots are the vertices of an extracted polygonal chain.

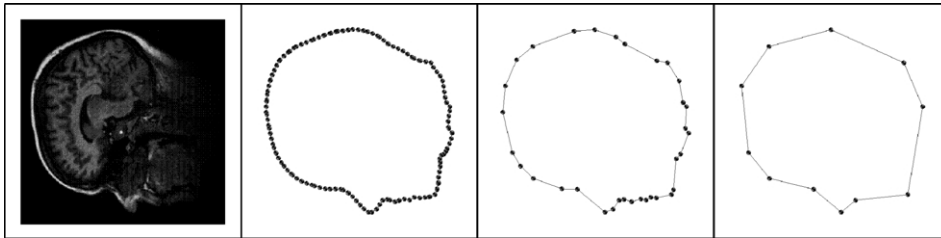


Fig. 2.3. From an image to polygonal chains.

c. Contour from an image

A 2D image can be treated as a piecewise C^0 bilinear function interpolating the intensity values at each pixel. A linear isocontour of the function is a polygonal chain. Of course, such a polygonal chain may be quite dense, hence a simplification step is often used to obtain coarser or multiresolution representations. Fig. 2.3 shows an image and an isocontour with two simplified polygonal chains. The simplification method is established based on geometric error (Euclidean distance) control, that is, a point is removed if the distance of the point to the line, that interpolates its two neighbor points, is less than a given ε . Hence all original points are within an ε -neighborhood of the simplified polygonal chain. Again, the G^1 D_3 -regular curves defined on rectangles with rectangle-width 2ε are just the right family of curves to provide smooth approximation of these polygonal chains. The two simplified polygonal chains in Fig. 2.3 are obtained by taking ε to be 0.05 and 0.25, respectively.

d. Polygonal chain to polygonal chain

One polygonal chain can be produced from another polygonal chain by subdivision or corner cutting. Fig. 2.4 shows four polygonal chains obtained by corner cutting with cutting ratios 0.25 and 0.5, respectively and subdivision. When the cutting ratio is 0.5, then each edge of the new polygonal chain is *convex* (see the next section for the definition of a *convex* edge) if the tangents at the vertices are taken to be the original edges. Smooth approximations of these polygonal chains are suitable for triangular A-splines (Bajaj and Xu, 1999) as well as our D_3 -regular curves (see Section 5.1). The vertices of the polygonal chain (c) are located away from the original edge by a specified distance δ . We call this an “offset corner cutting” scheme. The offset will make constructed D_4 -regular curves be in a bounded neighborhood of the original vertices and hence appropriate for over-sampled

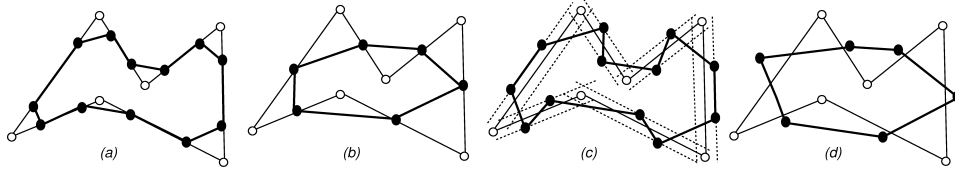


Fig. 2.4. Polygonal chains (of black vertices) produced from polygonal chains (of white vertices): (a) Corner cut with cutting ratio 0.25; (b) Corner cut with cutting ratio 0.5 yielding a convex polygon; (c) Offset corner cut with cutting ratio 0.25; (d) Interpolatory subdivision.

noisy vertex data. For the same purpose, an interpolatory subdivision scheme (see, e.g. (Warren, 1995)) could also be employed (see Fig. 2.4(d)) such as the 4-point rule with mask $(-1/16, 9/16, 9/16, -1/16)$ (see (Dyn et al., 1987)).

3. Some notations and preliminaries

Tensor BB form

The regular spline curve discussed in this paper consists of a chain of curve segments. Each segment is defined by the zero contour of a bivariate polynomial

$$G_{mn}(u, v) = \sum_{i=0}^m \sum_{j=0}^n b_{ij} B_i^m(u) B_j^n(v)$$

on a parallelogram $[p_1 p_2 p_3 p_4]$, where $(u, v)^T \in [0, 1] \times [0, 1]$ relates to a point $p = (x, y)^T \in [p_1 p_2 p_3 p_4]$ by the map

$$p = (p_3 - p_1)u + (p_2 - p_1)v + p_1. \quad (3.1)$$

We assume that p_1, p_2, p_4, p_3 are clockwise, any three of them are not collinear and $p_1 - p_2 = p_3 - p_4$. From map (3.1), we have

$$[u, v]^T = [p_3 - p_1, p_2 - p_1]^{-1}[p - p_1] = M[p - p_1].$$

Derivative data

A polygonal chain is denoted by its vertices $\{v_i\}_{i=0}^N$. On each vertex, we assume that the first (for G^1 continuity) and the second (for G^2 continuity) order derivatives are given. We assume these derivatives are the evaluation results of an (unknown) parametric form curve $r(l)$ at $l = l_i$. Hence these derivatives are plane vectors denoted by $r_i^{(j)} := r^{(j)}(l_i)$, $j = 1, 2$. These derivatives can be estimated from the given data by some known techniques, such as divided differences or local interpolation by parametric curve (see, for e.g., (Bajaj and Xu, 1999)). Other types of data, for instance functional curve data or implicitly defined curve data, could be converted to parametric data (see (Bajaj and Xu, 1999)). Furthermore, without loss of generality, we assume that the parameter l is the arc length of the curve. It is well known that, if l is the arc length of the curve, the derivative vectors have the following geometric interpretation: $r^{(1)}(l)$ is the tangent vector with unit length, $r^{(2)}(l)$ is the normal

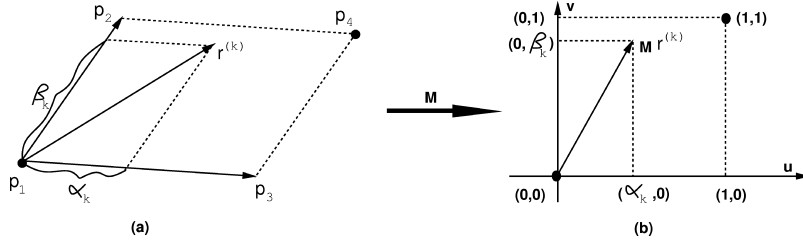


Fig. 3.1. (a) Decomposition of $r^{(k)}$ on $p_3 - p_1$ and $p_2 - p_1$; (b) The decomposition of $Mr^{(k)}$ in the local (u, v) system.

(i.e., $r^{(1)}(l)^T r^{(2)}(l) = 0$) and $\|r^{(2)}(l)\|$ is the curvature. If l is not the arc length, we can transform the derivatives by

$$\tilde{r}_i^{(1)} = r_i^{(1)} / \|r_i^{(1)}\|, \quad \tilde{r}_i^{(2)} = r_i^{(2)} / \|r_i^{(1)}\|^2 - (r_i^{(1)T} r_i^{(2)}) r_i^{(1)} / \|r_i^{(1)}\|^4$$

so that $\tilde{r}_i^{(1)}$ and $\tilde{r}_i^{(2)}$ have the required properties.

Decomposition of derivative data

Let $[p_1 p_2 p_3 p_4]$ be a parallelogram. Then we can decompose vectors $r^{(1)}(l)$ and $r^{(2)}(l)$ onto the direction $p_3 - p_1$ and $p_2 - p_1$ (see Fig. 3.1), i.e.,

$$r^{(k)}(l) = [p_3 - p_1, p_2 - p_1] [\alpha_k(l), \beta_k(l)]^T = M^{-1} [\alpha_k(l), \beta_k(l)]^T. \tag{3.2}$$

The decomposition coefficients $\alpha_k(l), \beta_k(l)$ will be frequently used later without further interpretation. It is easy to see that $\alpha_k(l) = 0$ if $r^{(k)}(l)$ is parallel to $p_2 - p_1$. Similarly, $\beta_k(l) = 0$ if $r^{(k)}(l)$ is parallel to $p_3 - p_1$. Using map (3.1) and decomposition (3.2), we may convert the curve construction problem on $[p_1 p_2 p_3 p_4]$ into that on $[0, 1] \times [0, 1]$ in the (u, v) -system.

G¹ and G² continuity

Let $G_{mn}(u, v) = 0$ be the curve defined on $[p_1 p_2 p_4 p_3]$. Suppose the curve is parameterized as $r(l)$. Then $H(l) := G_{mn}(u(l), v(l)) := G_{mn}(M[r(l) - p_1]) \equiv 0$. Differentiating $H(l) = 0$ about l once and twice, we have

$$r^{(1)}(l)^T M^T \nabla G_{mn} = 0, \tag{3.3}$$

$$r^{(2)}(l)^T M^T \nabla G_{mn} + r^{(1)}(l)^T M^T \nabla^2 G_{mn} M r^{(1)}(l) = 0, \tag{3.4}$$

where $\nabla G_{mn} = [\partial G_{mn} / \partial u, \partial G_{mn} / \partial v]^T$ and $\nabla^2 G_{mn} = \nabla(\nabla G_{mn})^T$. Condition (3.3) forces the curve $G_{mn}(u, v) = 0$ tangent with the curve $r(l)$, hence the curve is G^1 continuous if $\nabla G_{mn} \neq 0$. Condition (3.4) forces the curve $G_{mn}(u, v) = 0$ to be doubly tangent with the curve $r(l)$, hence the curve is G^2 continuous. Higher order continuity formulas can be derived by differentiating (3.4), but they will have more terms. In this paper, we consider only continuity up to G^2 . Using decomposition (3.2), (3.3) and (3.4) become

$$[\alpha_1(l), \beta_1(l)] \nabla G_{mn} = 0, \tag{3.5}$$

$$[\alpha_2(l), \beta_2(l)] \nabla G_{mn} + [\alpha_1(l), \beta_1(l)] \nabla^2 G_{mn} [\alpha_1(l), \beta_1(l)]^T = 0. \tag{3.6}$$

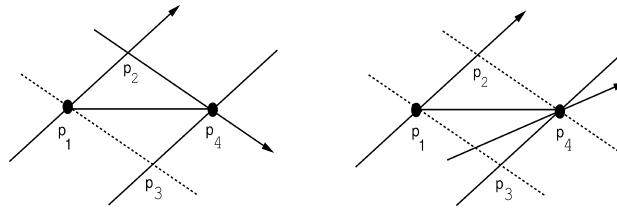


Fig. 3.2. Left: convex edge. Right: nonconvex edge. The lines with arrows are tangents.

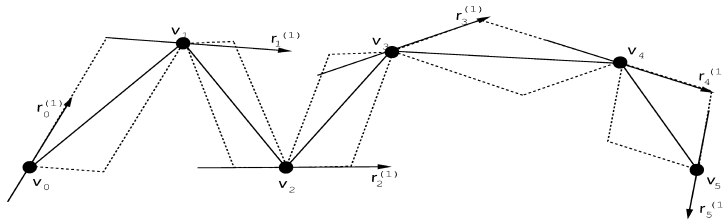


Fig. 4.1. Parallelogram chain.

In the next two sections, we shall use these relations to construct G^1 and G^2 curves.

Convexity of an edge

For an edge $[v_{i-1}v_i]$ of a polygon chain $\{v_i\}_{i=0}^N$, if the vectors $r_{i-1}^{(1)}$ and $r_i^{(1)}$ at v_{i-1} and v_i lie on opposite sides of the line $t(v_i - v_{i-1})$, then the edge is called *convex*. Otherwise it is *nonconvex* (see Fig. 3.2). In Fig. 4.1, $[v_0v_1]$, $[v_3v_4]$ and $[v_4v_5]$ are convex edges, $[v_1v_2]$ and $[v_2v_3]$ are nonconvex edges.

4. Polygonal chain approximation by D_4 -regular spline curves

Given an input polygonal chain $\{v_i\}_{i=0}^N$, we use D_4 -regular curves to smoothly approximate it, by interpolating the vertices with given first (for G^1 continuity) and the second (for G^2 continuity) order derivatives.

Step 1. Form a parallelogram chain

For each line segment (edge) of the polygonal chain, construct a parallelogram such that (see Fig. 4.1, where the arrows are tangent vectors): (i) the line segment is one of the diagonals of the parallelogram; (ii) the tangent line of a vertex is contained in the two incident parallelograms.

For a convex edge $[v_{i-1}v_i]$, the corresponding parallelogram can be formed by the four points p_2, v_{i-1}, p_3, v_i , where p_2 is the intersection point of the two tangents, $p_3 = v_{i-1} + v_i - p_2$. For a nonconvex edge, take one point on each side of the edge

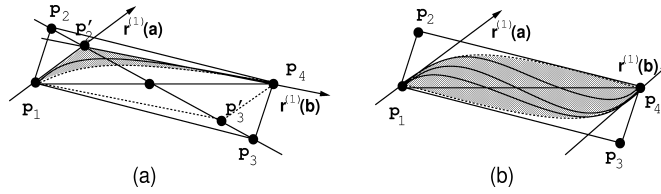


Fig. 4.2. (a) Symmetric parallelogram about the tangent and the curve family for a convex edge. The dotted curve is B_∞ . The shaded part is \mathcal{E}_1 ; (b) The curve family for a nonconvex edge. The dotted curves are L_0 and L_∞ . The shaded part is \mathcal{E}_2 .

such that $p_3 - v_{i-1} = v_i - p_2$. These two points and the endpoints of the edge form the parallelogram.

Assumption 4.1. For the convex edge $[v_{i-1}v_i]$, the tangent lines $v_{i-1} + sr_{i-1}^{(1)}$ and $v_i + tr_i^{(1)}$ have intersection point at (s^*, t^*) with $s^* > 0$.

It should be noted that under Assumption 4.1, it is always possible to construct a parallelogram chain, and that this construction is not unique. In the construction of G^1 curves for convex edges, we shall allow p_2 and p_3 to vary along a line (see Fig. 4.2(a) and relation (4.2) for varying p_2, p_3 that depend on a parameter λ). In other cases, these points are fixed.

Step 2. Construct D_4 -regular curves

For each parallelogram, construct a D_4 -regular curve, such that it interpolates the endpoints of the line segment and has the given first order or second order derivatives. Let $G_{mn}(u, v) = 0$ be the curve defined on $[p_1 p_2 p_3 p_4]$, where p_1 and p_4 are the interpolation points. In the following, we shall determine the minimal m and n , and provide the formulas for computing the coefficients of $G_{mn}(u, v)$ for G^1 and G^2 continuity. These formulas are derived using G^1 and G^2 conditions (3.5) and (3.6). The detailed algebraic derivation is given in Appendix A.

4.1. A G^1 curve spline family

A. Convex edge

Let $[p_1 p_4]$ be a convex edge, and $[p_1 p_2 p_3 p_4]$ be the parallelogram. Assume $p_1 = r(a), p_4 = r(b)$ for some a and b with $a < b$, and assume $\beta_1(a) > \alpha_1(a), \beta_1(b) < \alpha_1(b)$. Take $m = n = 1$.

1. Construction formulas.

$$b_{00} = b_{11} = 0, \quad b_{10} = 1, \quad b_{01} = \frac{1-\lambda}{\lambda} \in (-1, 0), \quad \lambda > 1, \quad (4.1)$$

$$p_2 = \lambda p_2' + (1-\lambda)p_3', \quad p_3 = (1-\lambda)p_2' + \lambda p_3', \quad (4.2)$$

where p_2' is the intersection point of the tangent lines of p_1 and p_4 (see Fig. 4.2(a)), $p_3' = p_1 + p_4 - p_2'$ and λ is a free parameter.

2. *Reformulation.* Let $p = (p'_3 - p_1)s + (p'_2 - p_1)t + p_1$. The curve $G_{11}(u, v) = 0$ could be redefined on the smaller parallelogram $[p_1 p'_2 p'_3 p_4]$ as:

$$B_\lambda: [4s - (s + t)^2]\lambda^2 - [4s - (s + t)^2]\lambda + s(1 - t) = 0. \tag{4.3}$$

3. *Bounding curves.* When $\lambda = 1$, the curve $G_{11}(u, v) = 0$ degenerates to straight lines $s = 0$ (the edge $[p_1 p'_2]$) and $t = 1$ (the edge $[p'_2 p_4]$), while when $\lambda = \infty$, the curve $G_{11}(u, v) = 0$ degenerates to the curve $B_\infty: 4s - (s + t)^2 = 0$.

4. *Interpolation of an interior point.* For any given point $p^* = (p'_3 - p_1)s^* + (p'_2 - p_1)t^* + p_1$ in the interior of the region \mathcal{E}_1 enclosed by the curves B_1 and B_∞ , there exists a unique $\lambda \in (1, \infty)$, that is

$$\lambda = \frac{1}{2} + \frac{t^* - s^*}{\sqrt{4s^* - (s^* + t^*)^2}}, \tag{4.4}$$

such that the curve $G_{11}(u, v) = 0$ interpolates the point p^* .

Theorem 4.1. *For a convex edge, there exists a degree (1, 1) ($m = n = 1$) D_4 -regular curve family $G_{11}(u, v) = 0$, defined by (4.1)–(4.2), with a free parameter $\lambda \in (1, \infty)$, in the region \mathcal{E}_1 enclosed by the curves B_1 and B_∞ . Each curve in the family G^1 interpolates the endpoints of the edge. For any given point p in the interior of \mathcal{E}_1 , there exists a unique curve, defined by (4.1)–(4.2) and (4.4), in this family that interpolates the point p .*

Note that the curve B_λ defined by (4.3) on $[p_1 p'_2 p'_3 p_4]$ is not in the form G_{11} . However, if we transform it into barycentric form on the triangle $[p_1 p'_2 p_4]$, then we can show that the curve is D_1 -regular on the triangle.

It is obvious that for fixed p_2 and p_3 that satisfy (4.2), there exists a unique curve $G_{11}(u, v) = 0$ that G^1 interpolates the edge.

Parameterization

From $G_{11}(u, v) = 0$, we obtain the parameterized expression

$$v = \frac{u}{u - b_{01}(1 - u)}, \quad u \in [0, 1].$$

B. Nonconvex edge

We assume $\beta_1(a) \geq \alpha_1(a)$, $\beta_1(b) \geq \alpha_1(b)$. Take $m = 1, n = 2$. If $\beta_1(a) \leq \alpha_1(a)$, $\beta_1(b) \leq \alpha_1(b)$, take $m = 2, n = 1$.

1. Construction formulas.

$$b_{00} = b_{12} = 0, \quad b_{10} = 1, \tag{4.5}$$

$$b_{01} = -\frac{1}{2}\delta \leq 0, \quad b_{11} = -\frac{1}{2}\gamma b_{02} > 0, \tag{4.6}$$

where $\delta = \alpha_1(a)/\beta_1(a)$, $\gamma = \alpha_1(b)/\beta_1(b)$ and $b_{02} < 0$ is a signed free parameter (see Fig. 4.2(b) for the curve family).

2. Bounding curves.

$$L_0: u(1-v) - \delta(1-u)v = 0,$$

$$L_{-\infty}: (1-u)v - \gamma u(1-v) = 0.$$

3. *Interpolation of an interior point.* For any given point $p = (u, v)^T$ in the interior of the region \mathcal{E}_2 enclosed by L_0 and $L_{-\infty}$, take

$$b_{02} = -\frac{(1-v)[u(1-v) - \delta(1-u)v]}{v[(1-u)v - \gamma v(1-v)]}, \quad (4.7)$$

then the curve determined by b_{02} interpolates the point p .

Theorem 4.2. *For a nonconvex edge, there exists a degree (1, 2) (or (2, 1)) D_4 -regular curve family, defined by (4.5)–(4.6) with a free parameter $b_{02} \in (0, -\infty)$, in the region \mathcal{E}_2 enclosed by L_0 and $L_{-\infty}$, whose members G^1 interpolate the endpoints of the edge. For any given point p in \mathcal{E}_2 , there exists a unique curve, defined by (4.5)–(4.7), in this family that interpolates the point p .*

Parameterization

Since $m = 1, n = 2$, the curve can be expressed in rational parameterized form

$$u = -\frac{b_{01}B_1^2(v) + b_{02}B_2^2(v)}{B_0^2(v) + (b_{11} - b_{01})B_1^2(v) - b_{02}B_2^2(v)}, \quad v \in [0, 1].$$

Shape control handles

For the given polygonal chain, the shape control handles are: (i) the direction of the tangent vector at each vertex; (ii) an interpolating point p in the region \mathcal{E}_1 , for convex edges, or \mathcal{E}_2 , for nonconvex edges.

4.2. A G^2 curve spline family

A. Convex edge

Let $[p_1 p_4]$ be a convex edge and $[p_1 p_2 p_3 p_4]$ be the parallelogram. Again, we assume $\beta_1(a) > \alpha_1(a)$, $\beta_1(b) < \alpha_1(b)$. Furthermore, we assume that the parallelogram is constructed so that $\alpha_1(a) = \beta_1(b) = 0$. Now we need to take $m = n = 2$.

1. Construction formulas.

$$b_{00} = b_{01} = b_{12} = b_{22} = 0, \quad b_{02} = -1, \quad (4.8)$$

$$b_{10} = \frac{\beta_1(a)^2}{\alpha_2(a)} > 0, \quad b_{21} = -\frac{\alpha_1(b)^2}{\beta_2(b)} > 0, \quad (4.9)$$

$$4b_{11} = 2b_{10} + 2b_{21} + 1 - b_{20}, \quad (4.10)$$

where b_{20} is a free parameter (see Fig. 4.3(a) for the curve family).

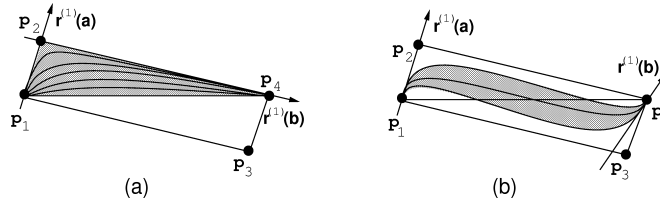


Fig. 4.3. (a) G^2 curve family for a convex edge. The shaded part is \mathcal{E}_3 ; (b) G^2 curve family for a nonconvex edge. The shaded part is \mathcal{E}_4 .

2. *Interpolation of an interior point.* Parameter b_{20} can be used to interpolate one point $(u, v)^T$ in the interior of the parallelogram with $u < v$. By $G_{22}(u, v) = 0$, we have

$$b_{20} = \frac{B_0^2(u)B_2^2(v) - b_{10}B_1^2(u)B_0^2(v) - [b_{21}B_2^2(u) + b_{11}B_1^2(u)]B_1^2(v)}{B_2^2(u)B_0^2(v)}. \quad (4.11)$$

3. *Reformulation.* Let $\alpha_1 = 1 - v$, $\alpha_2 = v - u$, $\alpha_3 = u$. Represent $G_{22}(u, v)$ in the barycentric coordinate form $\tilde{G}_{22}(\alpha_1, \alpha_2, \alpha_3)$ over the triangle $[p_1 p_2 p_4]$:

$$\tilde{G}_{22}(\alpha_1, \alpha_2, \alpha_3) := \sum_{i+j+k=3} a_{ijk} B_{ijk}^3(\alpha_1, \alpha_2, \alpha_3) \quad (4.12)$$

with

$$a_{300} = a_{210} = a_{003} = a_{012} = 0, \quad a_{111} = \frac{2b_{10} + 2b_{21} + b_{02} - b_{20}}{6}, \quad (4.13)$$

$$a_{201} = \frac{2}{3}b_{10}, \quad a_{102} = \frac{2}{3}b_{21}, \quad a_{120} = a_{021} = \frac{1}{3}b_{02}, \quad a_{030} = b_{02}. \quad (4.14)$$

Theorem 4.3. For a convex edge, say $[p_1 p_4]$, there exists a degree (2, 2) convex curve family in the triangle $\mathcal{E}_3 = [p_1 p_2 p_4]$, defined by (4.8)–(4.10), with b_{20} as a free parameter. Each member in the family G^2 interpolates the endpoints of the edge. If $b_{20} > 0$, the curve is D_4 -regular in the parallelogram $[p_1 p_2 p_4 p_3]$. If $b_{20} \leq 0$, the curve, that is re-defined by (4.12)–(4.14), is D_1 -regular on the triangle $[p_1 p_2 p_4]$. For any given point p in the interior of \mathcal{E}_3 , there exists a unique curve, defined by (4.8)–(4.11), in this family that interpolates the point p .

B. Nonconvex edge

Assume $\beta_1(a) \geq \alpha_1(a)$, $\beta_1(b) \geq \alpha_1(b)$ and the parallelogram is constructed so that $\alpha_1(a) = 0$ or $\alpha_1(b) = 0$. That is, at least one of the tangent lines at p_1 and p_4 coincides with one of the edges of the parallelogram (see Fig. 4.3(b)). Again, we take $m = n = 2$.

1. *Construction formulas.*

$$b_{00} = b_{22} = 0, \quad b_{01} = -\delta b_{10}, \quad b_{21} = -\gamma b_{12}, \quad (4.15)$$

$$4b_{11} = 2(b_{12} + b_{01} + b_{10} + b_{21}) - (b_{02} + b_{20}), \quad (4.16)$$

$$\begin{aligned}
b_{10} &= \frac{1}{\Delta} \{ \alpha_1(a) [\beta_1(a) - \alpha_1(a)] [\gamma\beta_2(b) - \alpha_2(b)] \\
&\quad + 2\alpha_1(a)\beta_1(a) [\beta_1(b) - \alpha_1(b)]^2 \} b_{20} \\
&\quad - \frac{1}{\Delta} \{ \beta_1(a) [\beta_1(a) - \alpha_1(a)] [\gamma\beta_2(b) - \alpha_2(b)] \} b_{02}, \tag{4.17}
\end{aligned}$$

$$\begin{aligned}
b_{12} &= \frac{1}{\Delta} \{ \alpha_1(b) [\beta_1(b) - \alpha_1(b)] [\alpha_2(a) - \delta\beta_2(a)] \\
&\quad + 2\alpha_1(b)\beta_1(b) [\beta_1(a) - \alpha_1(a)]^2 \} b_{02} \\
&\quad - \frac{1}{\Delta} \{ \beta_1(b) [\beta_1(b) - \alpha_1(b)] [\alpha_2(a) - \delta\beta_2(a)] \} b_{20}, \tag{4.18}
\end{aligned}$$

where $\delta = \alpha_1(a)/\beta_1(a)$, $\gamma = \alpha_1(b)/\beta_1(b)$, $\Delta = [\alpha_2(a) - \delta\beta_2(a)][\gamma\beta_2(b) - \alpha_2(b)]$, $b_{02} = -1$ and $b_{20} > 0$ is a free parameter (see Fig. 4.3(b) for the curve family).

2. Bounding curves. The bounding curves of the curve family are defined by taking $b_{20} = 0$ and $b_{20} = \infty$. Let $G_{22}(u, v, b_{02}, b_{20})$ be defined by (4.15)–(4.18). Then $G_{22}(u, v, b_{02}, 0) = b_{02}G_{22}(u, v, 1, 0)$, $G_{22}(u, v, 0, b_{20}) = b_{20}G_{22}(u, v, 0, 1)$. Hence the bounding curves are $G_{22}(u, v, 1, 0) = 0$, $G_{22}(u, v, 0, 1) = 0$.

Theorem 4.4. *For a nonconvex edge, we have a one parameter D_4 -regular curve family $\{b_{20}G_{22}(u, v, 0, 1) - G_{22}(u, v, 1, 0) = 0: b_{20} > 0\}$ whose members G^2 interpolate the edge and have only one inflection point. For any given point $p = (u^*, v^*)^T$ in the interior of the region \mathcal{E}_4 enclosed by the curves $G_{22}(u, v, 0, 1) = 0$ and $G_{22}(u, v, 1, 0) = 0$ in the parallelogram, there exists a unique curve in the family with $b_{20} = G_{22}(u^*, v^*, 1, 0)/G_{22}(u^*, v^*, 0, 1)$ that interpolates the point p .*

Curve evaluation and display

Since $G_{22}(u, v)$ could be expressed as $\sum_{i=0}^2 B_i(v)B_i^2(u)$ with $B_0(v) < 0$, $B_2(v) > 0$ on $(0, 1)$, the curve $G_{22}(u, v) = 0$ can be evaluated for each v in $(0, 1)$ by finding the zeros of a quadratic polynomial, here $B_i(v) = \sum_{j=0}^2 b_{ij}B_j^2(v)$. For the case of a convex edge, it is possible that the quadratic has two zeros in $(0, 1)$, and the correct one is such that $u < v$. For the nonconvex edge, the quadratic has exactly one zero in $(0, 1)$.

For intensive evaluation of the curve, the quarterly subdivision process for $G_{22}(u, v)$ on the rectangle $[0, 1] \times [0, 1]$ could be used (see (Peters, 1994)) while discarding those sub-rectangles on which the subdivision polynomials have only positive or negative coefficients. On each sub-rectangle, a bilinear function, that interpolates function values on the four vertices, is used to evaluate the curve intersection points. It follows from (Dahmen, 1986) that such a subdivision will have quadratic convergence. For example, ten steps of subdivision will reduce the distance between the polynomial and the BB net to become $(1/2^{10})^2 \approx 10^{-6}$ times the initial distance. By keeping a tree data structure, we achieve a progressive display scheme for our curve splines.

Shape control handles

For the given polygonal chain, the shape control handles of the curve are:

- (i) the direction of tangent vector at each vertex;

- (ii) the magnitude of the second order derivative vector (related to curvature) at each vertex;
- (iii) an interpolating point in the region \mathcal{E}_3 for convex edges, or \mathcal{E}_4 for nonconvex edges.

5. Polygonal chain approximation by D_3 -regular curves

We shall use D_3 -regular curves to smoothly approximate the polygon by interpolating the vertices together with the given tangents at the vertices. We could also interpolate second order derivatives at the polygon vertices to achieve G^2 continuity. Here we only detail G^1 continuity. The G^2 construction is very similar. The construction consists of the following two steps:

Step 1. Form a rectangular chain

For each line segment (edge) $[v_{i-1}v_i]$ of the polygonal chain, construct a rectangle such that (see Fig. 5.1, where the arrows are tangent vectors) the line segment is in the middle of the rectangle. That is, two edges are parallel to the line segment at an equal distance ε_i from it, and the other two edges are orthogonal to the line segment and pass through the endpoints of the line segment. Since the determined curve shall lie within the rectangle, ε_i serves as a natural error controller of the approximation. The effect of ε_i will be discussed further in Section 5.2.

Assumption 5.1. For each edge $[v_{i-1}v_i]$, $(v_i - v_{i-1})^T r_{i-1}^{(1)} > 0$, $(v_i - v_{i-1})^T r_i^{(1)} > 0$.

Step 2. Construct the D_3 -regular curves

For each rectangle, construct a D_3 -regular curve, such that it interpolates the endpoints of the line segment and has given first order derivatives. Let $[p_1 p_2 p_3 p_4]$ be a given rectangle, $v_0 = (p_1 + p_2)/2$, $v_1 = (p_3 + p_4)/2$ be the interpolation points and $r_0^{(1)}, r_1^{(1)}$ be the tangent vectors.

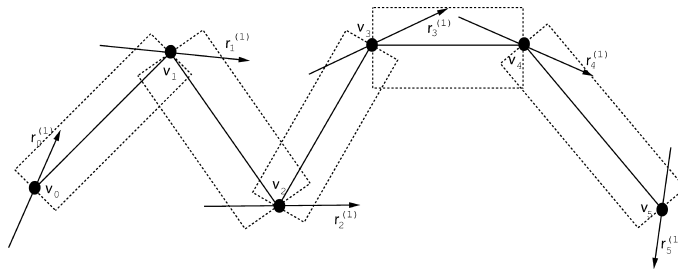


Fig. 5.1. Rectangular chain. The width of the rectangle for edge $[v_{i-1}v_i]$ is $2\varepsilon_i$.

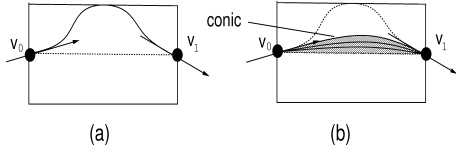


Fig. 5.2. (a) Nonconvex curve; (b) Convex curves (the solid curves). The shaded part is \mathcal{E}_5 .

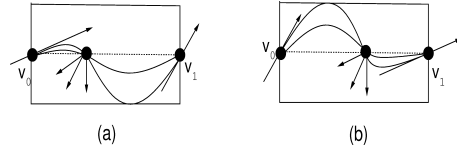


Fig. 5.3. (a) The case $\alpha \leq \beta$; (b) The case $\alpha > \beta$.

5.1. A G^1 curve spline family

A. Convex edge

Suppose $[v_0v_1]$ be a convex edge. From Assumption 5.1, we have $\alpha_1(a) > 0, \alpha_1(b) > 0$. Now assume $\beta_1(a) > 0, \beta_1(b) < 0$ (the case $\beta_1(a) < 0, \beta_1(b) > 0$ is similar) and take $m = 2, n = 1$.

1. Construction formulas.

$$b_{00} = 1, \quad b_{21} = -b_{20}, \quad b_{01} = -1, \quad (5.1)$$

$$b_{10} + b_{11} = 2\alpha = -2\beta b_{20}, \quad b_{20} = -\alpha\beta^{-1} > 0, \quad (5.2)$$

where $\alpha = \beta_1(a)/\alpha_1(a), \beta = \beta_1(b)/\alpha_1(b), b_{11}$ is a free parameter (see Fig. 5.2(b) for the curve family).

2. Limitations on free parameters. To make the curves D_3 -regular and convex, we enforce

$$b_{11} < b_{11}^* := \min \left\{ \sqrt{-\alpha\beta^{-1}}, -\frac{1}{2} + \alpha[1 + \beta^{-1}] \right\}. \quad (5.3)$$

Theorem 5.1. For a convex edge, let $G_{21}(u, v, b_{11})$ be defined by (5.1)–(5.2), then we have a convex D_3 -regular curve family $\{G_{21}(u, v, b_{11}) = 0: b_{11} < b_{11}^*\}$, whose members G^1 interpolate the endpoints of the edge. For any given point $p = (u^*, v^*)^T$ in the region \mathcal{E}_5 enclosed by the curve $G_{21}(u, v, b_{11}^*) = 0$ and the line $v = \frac{1}{2}$ there exists a unique b_{11} satisfying $G_{21}(u^*, v^*, b_{11}) = 0$ such that the curve $G_{21}(u, v, b_{11}) = 0$ interpolates the point p .

B. Nonconvex edge

Assume $\beta_1(a) \geq 0, \beta_1(b) \geq 0$. Take $m = 3, n = 1$.

1. Construction formulas.

$$b_{00} = b_{30} = 1, \quad b_{01} = b_{31} = -1, \quad (5.4)$$

$$b_{10} + b_{11} = \frac{4}{3}\alpha, \quad b_{20} + b_{21} = -\frac{4}{3}\beta, \quad (5.5)$$

$$b_{11} + b_{20} = b_{10} + b_{21}, \quad (5.6)$$

$$b_{10} = b_{20} + \frac{2}{3}(\alpha + \beta), \quad b_{21} = b_{11} - \frac{2}{3}(\alpha + \beta), \quad (5.7)$$

where $\alpha = \beta_1(a)/\alpha_1(a)$, $\beta = \beta_1(b)/\alpha_1(b)$, b_{20} or b_{11} is a free parameter (see Fig. 5.3 for the curve family).

2. *Limitations on free parameters.* To ensure the curves are D_3 -regular and have only one inflection point, we require

$$b_{20} > \max \left\{ b_{20}^*, \frac{\alpha - \beta - 2\alpha\beta}{3\alpha}, \frac{\beta - \alpha - 2\beta^2}{3\beta} \right\} \quad \text{when } \alpha \leq \beta, \quad (5.8)$$

$$b_{11} < \min \left\{ b_{11}^*, \frac{\beta - \alpha + 2\alpha^2}{3\alpha}, \frac{\alpha - \beta + 2\alpha\beta}{3\beta} \right\} \quad \text{when } \alpha > \beta, \quad (5.9)$$

where b_{20}^* is the largest negative root of $h(b_{20}) = 0$, b_{11}^* is the smallest positive root of $g(b_{11}) = 0$ with

$$\begin{aligned} h(b_{20}) &:= 1 + 4b_{10}^3 + 4b_{20}^3 - 3b_{10}^2b_{20}^2 - 6b_{10}b_{20}, \\ g(b_{11}) &:= 1 - 4b_{11}^3 - 4b_{21}^3 - 3b_{11}^2b_{21}^2 - 6b_{11}b_{21}. \end{aligned}$$

3. *Interpolation to a normal.* It should be noted that all the curves pass through the same point $(u^*, \frac{1}{2})^T$ with $u^* = \frac{\alpha}{\alpha + \beta}$ (see Fig. 5.3). Since

$$\nabla G_{31} \left(u^*, \frac{1}{2} \right) = \left[-\frac{2\alpha\beta}{\alpha + \beta}, -\frac{2(\alpha^3 + \beta^3)}{(\alpha + \beta)^3} - \frac{(6b_{20} + 4\beta)\alpha\beta}{(\alpha + \beta)^2} \right]^T,$$

by assigning a normal at $(u^*, \frac{1}{2})^T$, the unique b_{20} is determined.

Theorem 5.2. *For a nonconvex edge, there exists a D_3 -regular curve family $\{G_{31}(u, v) = 0\}$ that has the following properties:*

- (i) *Each curve in the family G^1 interpolates the edge.*
- (ii) *Each curve passes through the point $(u^*, \frac{1}{2})^T$.*
- (iii) *There is only one curve in that family that has the given normal at $(u^*, \frac{1}{2})^T$.*
- (iv) *The curve $v = \frac{1}{2}$ and the curve given by $b_{20} = b_{20}^*$ (if $\alpha \leq \beta$) or $b_{11} = b_{11}^*$ (if $\alpha > \beta$) are the two limit curves of the family.*

Parameterization

Since the curve is defined by $G_{m1}(u, v) = \sum_{i=0}^m b_{i0}B_i^m(u) + v \sum_{i=0}^m (b_{i0} - b_{i1})B_i^m(u) = 0$, it follows from (3.1) that

$$p = (p_3 - p_1)u - (p_2 - p_1) \frac{\sum_{i=0}^m b_{i0}B_i^m(u)}{\sum_{i=0}^m (b_{i0} - b_{i1})B_i^m(u)} + p_1, \quad u \in [0, 1].$$

5.1.1. *Shape control handles*

For the given polygonal chain, the shape control handles of the curve are: (i) the direction of the tangent vector at each vertex; (ii) an interpolating point in the region \mathcal{E}_5 , for convex edges, or a normal at $(u^*, \frac{1}{2})^T$, for nonconvex edges.

5.2. The effect of the size of rectangle

In the construction of rectangles in Step 1 at the beginning of this section, the widths of the rectangles, namely $2\varepsilon_i$, are arbitrarily chosen. One may ask: what is the effect of this ε_i on the constructed curves for a given edge $[v_{i-1}v_i]$? The conclusion is the following: *The curve family for smaller ε_i is a subset of the curve family for larger ε_i* , for each of the two cases discussed in Section 5.1. That is, ε_i will not change the shape of the curves but changes the “number” of curves in the family. When $\varepsilon_i > 0$ becomes successively smaller, more and more curves are expelled from the curve family, and the remaining curves (still infinitely many) are successively close to edge (see Figs. 6.1(c) and (d)). To prove this conclusion, suppose ε_i is magnified by a factor $\theta > 1$, and suppose the notation on the enlarged rectangle is the same as the original one but with an added prime. It is then easy to see that

$$\alpha'_1(l) = \alpha_1(l), \quad \beta'_1(l) = \theta^{-1}\beta_1(l), \quad u = u', \quad v = \theta\left(v' - \frac{1}{2}\right) + \frac{1}{2}.$$

Hence

$$B_0^1(v) = \frac{1}{2}(1 + \theta)B_0^1(v') + \frac{1}{2}(1 - \theta)B_1^1(v'),$$

$$B_1^1(v) = \frac{1}{2}(1 - \theta)B_0^1(v') + \frac{1}{2}(1 + \theta)B_1^1(v').$$

Substituting these into $G_{m1}(u, v)$, we have

$$G_{m1}(u, v) = \theta G'_{m1}(u', v') = \theta \sum_{i=0}^m \sum_{j=0}^1 b'_{ij} B_i^m(u') B_j^1(v')$$

with

$$b'_{i0} = \frac{(1 + \theta)b_{i0} + (1 - \theta)b_{i1}}{2\theta}, \quad b'_{i1} = \frac{(1 - \theta)b_{i0} + (1 + \theta)b_{i1}}{2\theta}.$$

Using these relations, we verify that b'_{ij} satisfies all the relations as b_{ij} does. Therefore, curve $G_{m1}(u, v) = 0$ defined on the smaller rectangle is in the curve family defined on the larger rectangle. Note that this statement holds for both the cases of the convex edge and the nonconvex edge discussed in Section 5.1.

Note

In the six spline families we discuss in Sections 4 and 5, there are four cases with $\min\{m, n\} = 1$. In these cases, rational parametric expressions are easily derived. Hence, for these cases, we have both the implicit form and the parametric form. For example, the $G^1 D_3$ -regular curve could be transformed into a parametric rational Bézier curve of degree 4. The right figure of Fig. 5.4 shows the Bézier points of a $G^1 D_3$ -regular curve as well as the rectangle chain for the input polygonal chain (right figure). It is clear that the rectangles enclose the curve more tightly than the convex hull of the Bézier points. Furthermore, the shape of curve is easier to control using its implicit form than using its parametric form, since the implicit form has one free parameter while the rational Bézier of degree 4 has many more degrees of freedom. Also, the parameter change of the rational Bézier form may lead the curve out of the $G^1 D_3$ -regular curve family.

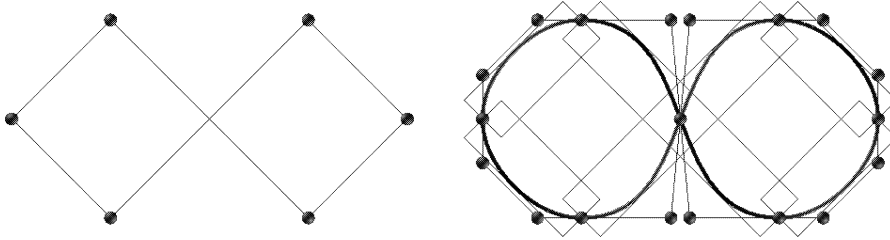


Fig. 5.4. The left figure shows the input polygon. The right shows the G^1 D_4 -regular curves and Bézier points interpolating the vertices of the polygon within prescribed bounds.

6. Examples

To illustrate the data fitting flexibility of the spline curves introduced in the last two sections, we provide several examples. In order to illustrate the features for each case, we use first the following regular data:

$$\begin{aligned} \{v_i\} &= \{(1, 1), (0, 2), (-1, 1), (1, -1), (0, -2), (-1, -1)\}, \\ \{r_i^{(1)}\} &= \{(0, 1), (-1, 0), (0, -1), (0, -1), (-1, 0), (0, 1)\}, \\ \{r_i^{(2)}\} &= \{(-1, 0), (0, -1), (1, 0), (-1, 0), (-1, 0), (1, 0)\}. \end{aligned}$$

In each case, ten curves are plotted (see Figs. 6.1(a)–(d)) for ten different parameters to show the curve family. The features of the curves shown in the figures coincide with the analysis in Sections 4 and 5.

For the convex edge, the G^1 curves (in Fig. 6.1(a)) within a parallelogram are located away from the convex edge. In contrast, the G^1 curves (Figs. 6.1(c), 6.1(d)) within a rectangle are located near the convex edge. The G^2 curve family within a parallelogram (Fig. 6.1(b)) has both these features.

For the nonconvex edge, the G^1 curves (in Fig. 6.1(a)) within a parallelogram tend to go directly from one vertex to the other. Hence the curves have sharp changes in the tangent direction at the end points for the parameters near the boundary of its domain, even though the curves are rather straight in the middle. The G^2 curves within a parallelogram (Fig. 6.1(b)) do not have sharp changes in the tangent direction. The G^1 curves (Figs. 6.1(c), 6.1(d)) within a rectangle closely follow the letter S, and additionally, all pass through the same point. The curves in Fig 6.1(d) are G^1 within the rectangle, but within a smaller size (width = $2\varepsilon_i$, and $\varepsilon_i = 0.2$, in contrast with $\varepsilon_i = 1.0$ in Fig. 6.1(c)) of rectangle. As one can observe, these curves shrink towards the edges of the shrunken rectangle.

In summary, D_3 -regular and D_4 -regular curves have several common features and have different features as well. For example, both of them can be sharp (rapid change of tangent line) at the vertices. However, D_4 -regular curves can also be very flat (slow change of tangent line) around vertices and sharp at other parts. D_3 -regular curves cannot be very flat around vertices if ε_i is small. These features can be utilized in shape design where sharp and flat features are required.

The features of the curves introduced in this paper strongly suggest that these tensor-product BB-form curve families serve a variety of geometric design and computer graphics

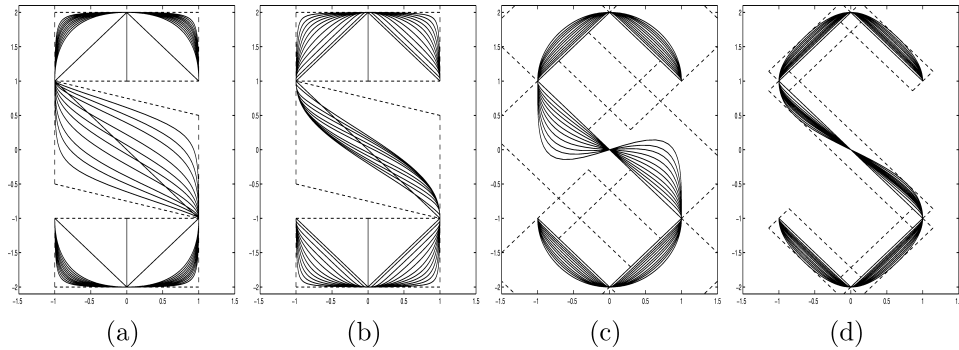


Fig. 6.1. (a) G^1 families on parallelograms. (b) G^2 families on parallelograms. (c) G^1 families on rectangles with $\varepsilon_i = 1.0$. (d) G^1 families on rectangles with $\varepsilon_i = 0.2$.

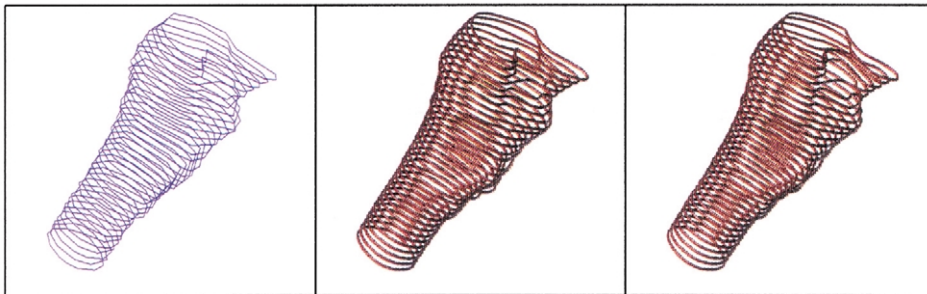


Fig. 6.2. The figure on the left shows a stack of input polygon contours of a human femur. The middle and right show the G^1 and G^2 D_4 -regular curves interpolating the vertices of the contours, respectively.

applications. Figs. 6.2 and 6.3 show some fitting examples from real data. Here the input data are normalized into the cube $[-3, 3]^3$. The polygonal chains in Fig. 6.2 (left) are the simplified contours stack of a human femur. Fig. 6.2 (middle and right) are the results of G^1 and G^2 D_4 -regular curve approximation. The polygonal chains in the first row of Fig. 6.3 are the simplified results of the polygonal chain shown in Fig. 2.3. The polygonal chains in the third row of Fig. 6.3 are three fonts. The second and fourth rows are the curve approximations.

7. Conclusions and future work

We have characterized the lowest bi-degree tensor BB-form polynomial to achieve G^1 and G^2 continuous regular algebraic spline curves. Using the lowest bi-degree, we constructed explicit spline curve families whose members satisfied given G^1 and G^2 interpolation conditions. We also derived a geometric interpretation of each spline curve family, so that the shape of the individual curves can be controlled intuitively.

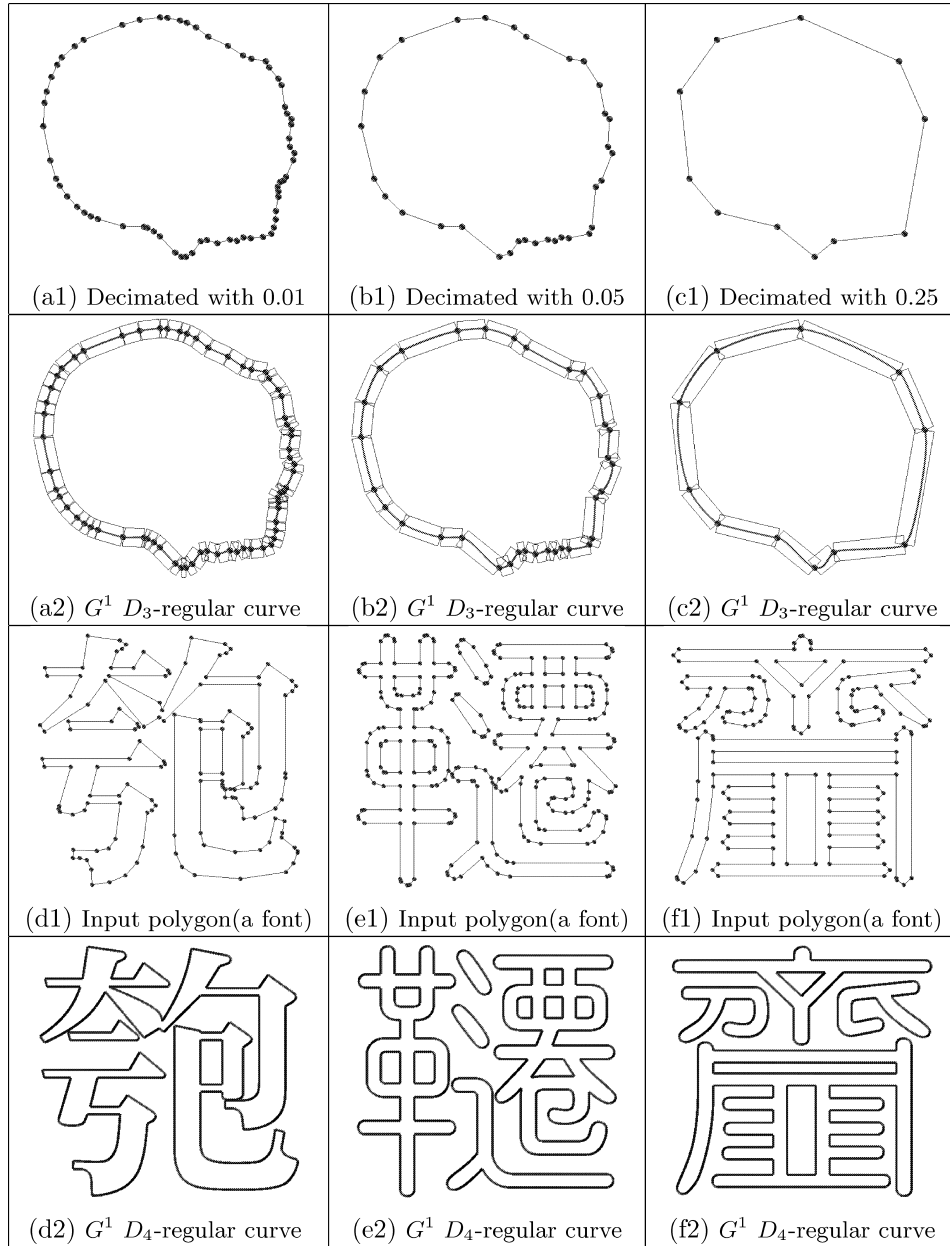


Fig. 6.3. The figures in the first row show the multiresolution representation of the input data with geometry errors 0.01, 0.05 and 0.25, respectively. The second row is the corresponding $G^1 D_3$ -regular curves with rectangle chains, where the width of the rectangles are chosen to be 0.3. The third and fourth rows are input polygons of three Chinese fonts and the corresponding $G^1 D_4$ -regular curves (with certain G^0 vertices to capture the sharp features of the fonts).

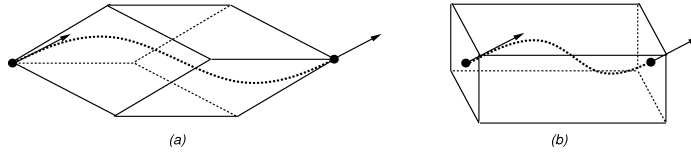


Fig. 7.1. Implicit space spline curve segment defined within (a) parallelepiped and (b) cubocoid, using dual trivariate tensor product polynomial functions in BB-form.

Finally, we point out that the D_3 and D_4 -regular curves used in this paper can be extended to 3D space curves. The parallelogram and the rectangle become the parallelepiped (see Fig. 7.1(a)) and the cubocoid (see Fig. 7.1(b)) volume cells, respectively. The G^1 and G^2 regular space spline curve segments are now defined by the intersection of two zero contours of trivariate tensor product polynomial functions in BB-form within each volume cell. Properties and data fitting schemes for these implicitly defined space curves are currently being researched.

Appendix A

Proof of Theorem 4.1. Let $[p_1 p_4]$ be a convex edge, and $[p_1 p_2 p_3 p_4]$ be the parallelogram that maps to the unit square by (3.1). Assume $p_1 = r(a)$, $p_4 = r(b)$ for some a and b with $a < b$. It is easy to see that (see Fig. 3.1) the edge is convex if and only if $\beta_1(a) > \alpha_1(a)$, $\beta_1(b) < \alpha_1(b)$ or $\beta_1(a) < \alpha_1(a)$, $\beta_1(b) > \alpha_1(b)$. Now we assume $\beta_1(a) > \alpha_1(a)$, $\beta_1(b) < \alpha_1(b)$ (for the other case the discussion is the same, in fact, we need only exchange the index of p_2 and p_3). Using the interpolation condition $G_{mn}(0, 0) = G_{mn}(1, 1) = 0$, we have

$$\nabla G_{mn}(0, 0) = [mb_{10}, nb_{01}]^T, \quad \nabla G_{mn}(1, 1) = -[mb_{m-1,m}, nb_{n,n-1}]^T. \quad (\text{A.1})$$

If we take $m = n = 1$, then by interpolating p_1 and p_4 and the normalization condition, we have (4.1) and then by (3.5) and (A.1) we have $\alpha_1(a) + \beta_1(a)b_{01} = 0$, $\alpha_1(b)b_{01} + \beta_1(b) = 0$. Hence $b_{01} = -\alpha_1(a)/\beta_1(a)$, $b_{01} = -\beta_1(b)/\alpha_1(b)$. Therefore, we require that

$$\alpha_1(a)\alpha_1(b) = \beta_1(a)\beta_1(b). \quad (\text{A.2})$$

Let $n_1 = -r^{(2)}(a)$ and $n_4 = -r^{(2)}(b)$ be the normal of $r(l)$. Then by (3.2) and the orthogonal condition $r^{(2)}(l)^T r^{(1)}(l) = 0$, we have

$$\begin{aligned} \alpha_1(a)n_1^T(p_3 - p_1) &= -\beta_1(a)n_1^T(p_2 - p_1), \\ \alpha_1(b)n_4^T(p_2 - p_4) &= -\beta_1(b)n_4^T(p_3 - p_4). \end{aligned}$$

Hence (A.2) holds if and only if

$$n_1^T(p_3 - p_1)n_4^T(p_2 - p_4) = n_1^T(p_2 - p_1)n_4^T(p_3 - p_4) \neq 0. \quad (\text{A.3})$$

This can be achieved if and only if $n_1^T(p_2 - p_1) > 0$ and the parallelogram is *symmetric* about the normals. That is, p_2 and p_3 are on the line $\langle \frac{p_1+p_4}{2}, p_2' \rangle$, where p_2' is the

intersection point of the tangent lines of p_1 and p_4 (see Fig. 4.2(a)). Let $p'_3 = p_1 + p_4 - p'_2$. Then there exists a $\lambda > 1$ such that

$$p_2 = \lambda p'_2 + (1 - \lambda)p'_3, \quad p_3 = (1 - \lambda)p'_2 + \lambda p'_3. \tag{A.4}$$

Substituting p_2 and p_3 into (A.3) and noting that $n_1^T(p'_2 - p_1) = 0$ and $n_4^T(p'_2 - p_4) = 0$, we can show that Eq. (A.3) holds, and

$$b_{01} = \frac{1 - \lambda}{\lambda}. \tag{A.5}$$

That is, $b_{01} \in (-1, 0)$ when $\lambda \in (1, \infty)$. Let $p = (p'_3 - p_1)s + (p'_2 - p_1)t + p_1$. Then by (3.1) and (A.4) we have

$$\begin{cases} s = \lambda u + (1 - \lambda)v \\ t = (1 - \lambda)u + \lambda v \end{cases} \quad \text{or} \quad \begin{cases} u = \frac{\lambda s + (\lambda - 1)t}{\lambda + \lambda - 1} \\ v = \frac{(\lambda - 1)s + \lambda t}{\lambda - 1 + \lambda} \end{cases}. \tag{A.6}$$

It follows from (A.5) and (A.6) that the curve $G_{11}(u, v) = b_{01}B_0^1(u)B_1^1(v) + B_1^1(u)B_0^1(v) = 0$ can be rewritten as

$$B_\lambda: [4s - (s + t)^2]\lambda^2 - [4s - (s + t)^2]\lambda + s(1 - t) = 0.$$

When $\lambda = 1$, the curve $G_{11}(u, v) = 0$ degenerates to the straight lines $s = 0$ and $t = 1$, while $\lambda = \infty$, the curve $G_{11}(u, v) = 0$ degenerates to the curve $B_\infty: 4s - (s + t)^2 = 0$. Hence if we allow the points p_2 and p_3 to vary along the line $\langle p'_2 p'_3 \rangle$, that is, λ varies in $(1, \infty)$, then we have a curve family between the limit curves B_1 and B_∞ with λ as parameter. For any given point $p^* = (p'_3 - p_1)s^* + (p'_2 - p_1)t^* + p_1$ in the interior of the region \mathcal{E}_1 enclosed by the curves B_1 and B_∞ (that is $4s^* - (s^* + t^*)^2 > 0, 0 < s^* < 1, 0 < t^* < 1$), there exists a unique $\lambda \in (1, \infty)$ defined by (4.4) such that the curve $G_{11}(u, v) = 0$ interpolates the point p^* . \square

Proof of Theorem 4.2. It is easy to see that the edge is nonconvex if and only if $\beta_1(a) \geq \alpha_1(a)$, $\beta_1(b) \geq \alpha_1(b)$ or $\beta_1(a) \leq \alpha_1(a)$, $\beta_1(b) \leq \alpha_1(b)$. We assume $\beta_1(a) \geq \alpha_1(a)$, $\beta_1(b) \geq \alpha_1(b)$. As for the convex edge case, we are lead to requirement (A.2) if $m = n = 1$. This equality contradicts the nonconvex assumption. Hence we take $m = 1, n = 2$. If $\beta_1(a) \leq \alpha_1(a)$, $\beta_1(b) \leq \alpha_1(b)$ we take $m = 2, n = 1$ and the discussion is similar. Then by the interpolation condition and the normalization condition, we have (4.5). Relation (4.6) follows from (3.5) and (A.1), where $b_{02} < 0$ is a free parameter. Therefore, we have a D_4 -regular curve family with $b_{02} \in (0, -\infty)$, whose members G^1 interpolate the endpoints. When $b_{02} = 0, b_{02} = -\infty$ the limit curves are

$$L_0: u(1 - v) - \delta(1 - u)v = 0, \quad L_{-\infty}: (1 - u)v - \gamma u(1 - v) = 0.$$

Both L_0 and $L_{-\infty}$ are conics and each of them G^1 interpolates one endpoint and G^0 interpolates the other. For any given point $p = (u, v)^T$ in the interior of the region \mathcal{E}_2 enclosed by L_0 and $L_{-\infty}$, there is a unique b_{02} defined by (4.7) such that the curve determined by b_{02} interpolates the point p . \square

Proof of Theorem 4.3. Let $[p_1 p_4]$ be a convex edge and $[p_1 p_2 p_3 p_4]$ be the parallelogram. Again, we assume $\beta_1(a) > \alpha_1(a)$, $\beta_1(b) < \alpha_1(b)$. Furthermore, we assume that the

parallelogram is constructed so that $\alpha_1(a) = \beta_1(b) = 0$. Now we need to take $m = n = 2$. Since

$$\nabla G_{22}(0, 0) = \begin{bmatrix} b_{10} \\ b_{01} \end{bmatrix}, \quad \nabla G_{22}(1, 1) = -2 \begin{bmatrix} b_{12} \\ b_{21} \end{bmatrix}, \quad (\text{A.7})$$

$$\nabla^2 G_{22}(0, 0) = 2 \begin{bmatrix} b_{20} - 2b_{10} & 2(b_{11} - b_{01} - b_{10}) \\ 2(b_{11} - b_{01} - b_{10}) & b_{02} - 2b_{01} \end{bmatrix}, \quad (\text{A.8})$$

$$\nabla^2 G_{22}(1, 1) = 2 \begin{bmatrix} b_{02} - 2b_{12} & 2(b_{11} - b_{21} - b_{12}) \\ 2(b_{11} - b_{21} - b_{12}) & b_{20} - 2b_{21} \end{bmatrix}, \quad (\text{A.9})$$

we have, from the interpolation and normalization conditions and (3.5)–(3.6), relations (4.8) and (4.9). Note that $\alpha_2(a) > 0$, $\beta_2(b) < 0$. Now b_{11} and b_{20} are free. One way to choose them is to take $b_{20} = 1$, hence the curve is D_4 -regular for any b_{11} . This parameter could be used to interpolate any single point in the interior of the parallelogram. However, the resulting curve may not be convex. If we require the curve be convex (note the edge is convex), we assume the curve is cubic. That is, the leading coefficient of $G_{22}(u, v)$ is zero which gives (4.10). Now we have a one parameter curve family, whose member G^2 interpolates the edge, with b_{20} being the free parameter. This degree of freedom can be used to interpolate one point $(u, v)^T$ in the interior of the parallelogram with $u < v$. That is, take b_{20} as (4.11).

It is easy to see that if $b_{20} > 0$, the curve is D_4 -regular. In the following we shall show that if $b_{20} \leq 0$, then the curve is D_1 -regular in the triangle $[p_1 p_2 p_4]$. Let $(\alpha_1, \alpha_2, \alpha_3)^T$ be the barycentric coordinate of $(u, v)^T$ in the triangle $[p_1 p_2 p_4]$. Then $\alpha_1 = 1 - v$, $\alpha_2 = v - u$, $\alpha_3 = u$. Represent $G_{22}(u, v)$ in the barycentric coordinate form $\tilde{G}_{22}(\alpha_1, \alpha_2, \alpha_3)$ over the triangle $[p_1 p_2 p_4]$:

$$\tilde{G}_{22}(\alpha_1, \alpha_2, \alpha_3) := \sum_{i+j+k=3} a_{ijk} B_{ijk}^3(\alpha_1, \alpha_2, \alpha_3),$$

we get (4.13)–(4.14). Hence $a_{201} > 0$, $a_{102} > 0$, $a_{120} < 0$, $a_{021} < 0$ and $a_{030} < 0$. Therefore, $\tilde{G}_{22}(\alpha_1, \alpha_2, \alpha_3) = 0$ is D_1 -regular. If $b_{20} \rightarrow \infty$, the curve degenerates to boundary lines of $[p_1 p_2 p_4]$. \square

Proof of Theorem 4.4. Since the edge is nonconvex, we have $\beta_1(a) \geq \alpha_1(a)$, $\beta_1(b) \geq \alpha_1(b)$ or $\beta_1(a) \leq \alpha_1(a)$, $\beta_1(b) \leq \alpha_1(b)$. Now we assume $\beta_1(a) \geq \alpha_1(a)$, $\beta_1(b) \geq \alpha_1(b)$ and the parallelogram is constructed so that $\alpha_1(a) = 0$ or $\alpha_1(b) = 0$. Again, we take $m = n = 2$ and the interpolation implies that $b_{00} = b_{22} = 0$. It follows from (3.5)–(3.6) and (A.7)–(A.9) that

$$b_{01} = -\delta b_{10}, \quad b_{21} = -\gamma b_{12}, \quad (\text{A.10})$$

$$\alpha_2(a)b_{10} + \beta_2(a)b_{01} + \alpha_1(a)^2(b_{20} - 2b_{10}) + 4\alpha_1(a)\beta_1(a)(b_{11} - b_{01} - b_{10}) + \beta_1(a)^2(b_{02} - 2b_{01}) = 0, \quad (\text{A.11})$$

$$-\alpha_2(b)b_{12} - \beta_2(b)b_{21} + \alpha_1(b)^2(b_{02} - 2b_{12}) + 4\alpha_1(b)\beta_1(b)(b_{11} - b_{21} - b_{12}) + \beta_1(b)^2(b_{20} - 2b_{21}) = 0, \quad (\text{A.12})$$

where $\delta = \alpha_1(a)/\beta_1(a)$, $\gamma = \alpha_1(b)/\beta_1(b)$. Again, we assume $G_{22}(u, v)$ is cubic. That is, the leading coefficient is zero, which yields

$$4b_{11} = 2(b_{12} + b_{01} + b_{10} + b_{21}) - (b_{02} + b_{20}). \tag{A.13}$$

Substituting (A.10) and (A.13) into (A.11) and (A.12) and then solving (A.11) and (A.12) for the unknowns b_{10} and b_{12} , we have (4.17) and (4.18), where b_{02} and b_{20} are free parameters. From the construction of the parallelogram chain and the assumptions on the derivatives we know that

$$\alpha_2(a) - \delta\beta_2(a) > 0, \quad \gamma\beta_2(b) - \alpha_2(b) > 0.$$

Hence $\Delta > 0$ and $b_{10} > 0, b_{12} < 0$ if $b_{02} < 0, b_{20} > 0$. It follows from (A.10) that $b_{01} \leq 0, b_{21} \geq 0$. Hence the curve is D_4 -regular. Since the total degree of G_{22} is three, the curve has only one inflection point. By normalizing b_{02} to be -1 , we have one free parameter. \square

Proof of Theorem 5.1. Suppose $[v_0v_1]$ is a convex edge. As (3.2), let $r^{(1)} = \alpha_1(p_3 - p_1) + \beta_1(p_2 - p_1)$. From the construction of the rectangular chain, we have $\alpha_1(a) > 0, \alpha_1(b) > 0$. Now assume $\beta_1(a) > 0, \beta_1(b) < 0$ (the case $\beta_1(a) < 0, \beta_1(b) > 0$ is similar) and take $m = 2, n = 1$. Then from the G^0 and normalization conditions we have (5.1). Since

$$\nabla G_{21}\left(0, \frac{1}{2}\right) = [b_{10} + b_{11}, 2b_{01}]^T, \quad \nabla G_{21}\left(1, \frac{1}{2}\right) = -[b_{10} + b_{11}, 2b_{20}]^T,$$

(3.5) gives $b_{10} + b_{11} = 2\alpha = -2\beta b_{20}$, where $\alpha = \beta_1(a)/\alpha_1(a), \beta = \beta_1(b)/\alpha_1(b)$. Then we have (5.2). Hence we get a curve family with b_{11} as a free parameter. In order to have the curve to be D_3 -regular, we require (see Lemma 2.3 of (Xu et al., 2000b))

$$b_{11} < \sqrt{b_{01}b_{21}} = \sqrt{b_{20}} = \sqrt{-\alpha\beta^{-1}}.$$

Then by $b_{10} = -b_{11} + 2\alpha > -\sqrt{-\alpha\beta^{-1}} = -\sqrt{b_{00}b_{20}}$, the curve is D_3 -regular. However, the curve may not be convex (see Fig. 5.2(a)). If we further enforce (5.3), then the curve is convex. In fact, when $b_{11} = -\frac{1}{2} + \alpha [1 + \beta^{-1}]$, the curve is a conic and hence convex. When b_{11} satisfies (5.3), then the curve is below this conic curve (see Fig 5.2(b)) and again the curve is convex (see Theorem 3.1 of (Bajaj and Xu, 1999)). \square

Proof of Theorem 5.2. Assume $\beta_1(a) \geq 0, \beta_1(b) \geq 0$ (the case $\beta_1(a) \leq 0, \beta_1(b) \leq 0$ is similar) and take $m = 3, n = 1$. Note that the curve will intersect the line $v = \frac{1}{2}$ at least three times, hence $m = 3$ is the minimal degree in u . Take $b_{00} = b_{30} = 1, b_{01} = b_{31} = -1$, then the G^0 condition is satisfied. Since

$$\nabla G_{31}\left(0, \frac{1}{2}\right) = \left[\frac{3}{2}(b_{10} + b_{11}), -2\right]^T, \\ \nabla G_{31}\left(1, \frac{1}{2}\right) = \left[-\frac{3}{2}(b_{20} + b_{21}), -2\right]^T,$$

condition (3.5) yields (5.5). Again, we assume the leading coefficient of $G_{31}(u, v)$ is zero, which leads to (5.6). Hence we have (5.7). It follows from Lemma 2.4 of (Xu et al., 2000b) that the considered curve is D_3 -regular if and only if

$$h(b_{20}) := 1 + 4b_{10}^3 + 4b_{20}^3 - 3b_{10}^2b_{20}^2 - 6b_{10}b_{20} > 0,$$

$$g(b_{11}) := 1 - 4b_{11}^3 - 4b_{21}^3 - 3b_{11}^2b_{21}^2 - 6b_{11}b_{21} > 0.$$

Let b_{20}^* be the largest negative root of $h(b_{20}) = 0$, b_{11}^* be the smallest positive root of $g(b_{11}) = 0$. Then it is easy to check that if

$$b_{20} > b_{20}^*, \quad \text{when } \alpha \leq \beta; \quad \text{or } \quad b_{11} < b_{11}^*, \quad \text{when } \alpha > \beta, \quad (\text{A.14})$$

the curve is D_3 -regular. Furthermore, it should be noted that all the curves pass through the same point $(u^*, \frac{1}{2})^T$ with $u^* = \frac{\alpha}{\alpha+\beta}$ (see Fig. 5.3). Since

$$\nabla G_{31}\left(u^*, \frac{1}{2}\right) = \left[-\frac{2\alpha\beta}{\alpha+\beta}, -\frac{2(\alpha^3+\beta^3)}{(\alpha+\beta)^3} - \frac{(6b_{20}+4\beta)\alpha\beta}{(\alpha+\beta)^2} \right]^T,$$

by assigning a normal at $(u^*, \frac{1}{2})^T$, the unique b_{20} is determined. If b_{20} or resulting b_{11} satisfy (A.14), then the curve is D_3 -regular. To ensure that the curve has a minimal number of inflection points, we require that the curve is below the tangent line $v_0 + tr_0^{(1)}$ and is above the tangent line $v_1 + tr_1^{(1)}$. On the line $v_0 + tr_0^{(1)}$, $G_{31}(u, v)$ is a polynomial of degree 3 with the constant and linear terms being zero, since the curve is tangent with the line. From this we get $2(\alpha - \beta) + 3\alpha(b_{11} - b_{10}) < 0$. Substituting the second tangent line into $G_{31}(u, v)$, we obtain $2(\alpha - \beta) + 3\beta(b_{20} - b_{21}) > 0$. Using (5.5) and (5.6), we obtain

$$\begin{aligned} b_{11} &< \frac{\beta - \alpha + 2\alpha^2}{3\alpha}, & b_{20} &> \frac{\alpha - \beta - 2\alpha\beta}{3\alpha}, \\ b_{20} &> \frac{\beta - \alpha - 2\beta^2}{3\beta}, & b_{11} &< \frac{\alpha - \beta + 2\alpha\beta}{3\beta}. \end{aligned}$$

Combining these with (A.14), we have (5.8) and (5.9). \square

References

- Bajaj, C., Xu, G., 1999. A-splines: local interpolation and approximation using C^k -continuous piecewise real algebraic curves. *Computer Aided Geometric Design* 16, 557–578.
- Bhaskaran, V., Natarajan, B., Konstantinides, K., 1993. Optimal piecewise-linear compression of images, in: Cohn, M., Storer, J. (Eds.), *Proc. 1993 Data Compression Conference*, IEEE Computer Society Press, pp. 168–177.
- Dahmen, W., 1986. Subdivision algorithm converge quadratically. *J. Comput. Appl. Math.* 16, 145–158.
- Dyn, N., Gregory, J., Levin, D., 1987. A 4-point interpolatory subdivision scheme for curve design. *Computer Aided Geometric Design* 4, 257–268.
- Kass, M., Witkin, A., Terzopoulos, D., 1988. Snakes: active contour models. *Internat. J. Comput. Vision*, 321–331.
- Peters, J., 1994. Evaluation and approximate evaluation of the multivariate Bernstein–Bézier form on a regularly partitioned simplex. *ACM Trans. Math. Software* 20 (4), 460–480.
- Sethian, J.A., 1996. *Level Set Methods*. Cambridge University Press, Cambridge.
- Warren, J., 1995. Binary subdivision schemes for functions over irregular knot sequences, in: Dahlen, M., Lyche, T., Schumaker, L.L. (Eds.), *Mathematical Methods for Curves and Surfaces*, Vanderbilt University Press, Nashville, pp. 543–562.

- Xu, G., Bajaj, C., Chu, C., 2000a. Regular algebraic curve segments(II)—interpolation and approximation. *Computer Aided Geometric Design* 17, 503–519.
- Xu, G., Bajaj, C., Xue, W., 2000b. Regular algebraic curve segments(I)—definition and characteristics. *Computer Aided Geometric Design* 17, 485–501.